



OPEN Phytoliths of bamboo affect the feeding pattern of Giant panda (*Ailuropoda melanoleuca*)

Janika Tikka¹✉, Juha Varrela², Jorma Määttä³, Jukka Salo⁴, Hemin Zhang^{5,6,7}, Pekka Niemelä¹, Marko Haapakoski⁸ & Pekka K. Vallittu^{1,9}

Giant panda's evolutionary adaptation for using bamboo as food has been demonstrated by the morphology of premolars, and by the anatomy and function of the temporomandibular joint. Pandas feed on the leaves, limbs and stem of bamboo containing phytoliths. We characterized phytoliths of two bamboo species in order to determine which parts of bamboo could contain wear-causing phytoliths and to explain panda feeding behavior to remove the cortex of the stem of bamboo before eating. Two bamboo species (*Phyllostachys aureosulcata* and *Phyllostachys bissetii*) were characterized for their inorganic content, morphological chemical and microhardness. Analysis showed that there were less inorganic minerals in the stem than in the leaves of both bamboo species. Particle size of inorganic substance was larger in the leaves and they were classified to phytoliths whereas minerals in the cortex of stem were of nanometer scale. Mean wt% of inorganic substance in leaves was 6.9% and of cortex 1.1%. Phytoliths sizes in the leaves were 30–40 µm in diameter. Amorphous silica was the major oxide. Microhardness of the outer surface of the cortex, was higher than in the subcortical layer. Panda's feeding behavior, involving the removal of stem cortex may relate to the physical properties of the cortex. Synergistic causative factor of tooth wear may exist.

Enamel, the outermost layer of tooth crown with the most highly mineralized tissue in mammals, plays a critical role in biting function and protection of teeth from mechanical damage of fracture and wear. Giant pandas (*Ursidae*, *Ailuropoda melanoleuca* David 1869), inhabiting the mountain ranges of Central China (mainly Sichuan, Shaanxi and Gansu), feed, unlike other bears, almost exclusively on bamboo (*Poaceae: Bambusoidea*). There are several bamboo species which are grown for the diet of giant pandas in zoos in Europe.

Giant pandas have an evolutionary adaptation for consuming cellulose and silica-rich food. This has been demonstrated recently by the morphology of the teeth and by the anatomy and function of the temporomandibular joint^{1–4}. Pandas feed on the both leaves, limbs and stem of bamboo, although the stem of bamboo is known for high strength and toughness^{5,6}. The micro structure and mechanical properties of panda teeth are able to resist biting-force related fractures⁷. When tooth wear is considered, it is known that the surface hardness of panda tooth enamel is 3.37 GPa, corresponding to the surface hardness of human enamel (3.2 GPa)^{7,8} and that wear can be caused by exogenous and endogenous abrasives. A specific feeding pattern is the panda's habit to remove the outer layer (cortex) from the stalk of bamboo before eating. The lateral movement of the lower jaw and morphology of the teeth, especially premolars P3 and P4 have adapted for this function⁴. It has been suggested that the function of skimming the cortex of the stem of bamboo to be either related to the elimination of wear-causing silica particles in the cortex, or to avoid possible toxic cyanide compounds present in some bamboo species^{8–11}. Silica particles are hard mineral compounds, and their abrasive effect to the teeth of giant panda may be an important evolutionary factor behind the function of skimming the cortex of bamboo before eating. Silica appears to be the primary mode of defence against mammalian herbivore damage in graminoids (*Poaceae*) including bamboos^{12–14}. The hardness of the stem of bamboo species upon which giant pandas feed, has been

¹Department of Biomaterials Science and Turku Clinical Biomaterials Centre, Institute of Dentistry, University of Turku, Lemminkäisenkatu 2, 20520 Turku, Finland. ²Department of Pediatric Dentistry and Orthodontics, Institute of Dentistry, University of Turku, Turku, Finland. ³Institute of Biomedicine, Faculty of Medicine, University of Turku, Turku, Finland. ⁴Biodiversity Unit, University of Turku, Turku, Finland. ⁵China Conservation and Research Center for Giant Panda, Du Jiangyan, Sichuan, China. ⁶Key Laboratory of State Forestry and Grassland Administration on Conservation Biology of Rare Animals in the Giant Panda National Park, Du Jiangyan, Sichuan, China. ⁷Qionglai Mountains Conservation Biology of Endangered Wild Animals and Plants National Permanent Scientific Research Base, Du Jiangyan, Sichuan, China. ⁸Ähtäri Zoo, Ähtäri, Finland. ⁹Welfare District of South-West Finland, Turku, Finland. ✉email: janika.s.tikka@utu.fi

studied for the species *Phyllostachys nigra* and *Phyllostachys bissetii* but differences in the cortex, i.e. the part which the panda does not eat, and the subcortical part is not known¹⁵.

Silica as the major mineral may accumulate into plant tissue as deposits called phytoliths, which greatly increase the hardness and abrasiveness of plant material^{16,17}. Silica concentrations in leaves are typically as high as 10% of dry weight^{18,19}, which inhibits both feeding and digestibility by mammalian grazers¹⁷. Phytoliths are created when predominantly silica minerals are dissolved in soil in the presence of water. Released silicate ions in water are then absorbed through the roots of a plant and carried throughout its vascular system. In the global silicon cycle, silicate ions are precipitated in the various structures of the plant: in the lumina, cell walls, and intercellular spaces^{20,21}. Phytoliths are more commonly found in aerial structures of a plant than in its subterranean organs²¹. Furthermore, it has also been shown that the silicate ion concentration of grasses is inducible, increasing potentially up to four-fold in response to herbivory^{14,17}.

Morphologically, phytoliths in grass are mineral particles up to 10–20 µm in size or particle aggregates with a size of up to 500 µm and can potentially be abrasive for teeth^{22,23}. Attention has been paid to phytoliths of bamboo species and their relationship to tooth wear in herbivore primates including the extinct primate *Gigantopithecus blacki* and Giant Panda^{7,21}. Signs of occlusal microwear patterns were demonstrated in the molars of *Gigantopithecus blacki* with a diet of fruits and leaves²¹.

Recently, a more detailed analysis of the mechanisms of tooth wear among giant panda was made by investigating the enamel structure and its physical properties and some mesoscale physical properties of bamboo leaves and stems²⁴. Whether the phytoliths in the stem cortex and leaves of bamboo differ in their phytolith particle size and surface hardness, and whether these differences point toward a possible evolutionary explanation for the feeding behavior of giant panda is still unknown. Thus, in this study we characterized phytolith morphology and particle size, chemical composition and surface microhardness, especially hardness in different parts of the stem of two bamboo species. This characterization was done to find out whether the presence of phytoliths could explain panda feeding behavior of skimming the outer skin of bamboo before eating.

Materials and methods

Two bamboo species known to be consumed by giant panda, namely *Phyllostachys aureosulcata* (PA) and *Phyllostachys bissetii* (PB) were selected for this study. *Phyllostachys* bamboo species are common in the diet of giant panda and widely used as their food in zoos²⁵. Permission to use bamboo in this study was obtained from Bamboo Giant Nederland BV (Asten, Netherlands). The bamboos were cultured by the Bamboo Giant Nederland BV (Asten, Netherlands) in sandy well moistened soil and fields with clay soil with yearly addition of 400 kg/hectare of Monterra 9-7-1 nutrition (MeMon BV, Arnhem, Netherlands) with a composition of N 9%; P₂O₅ 7%; K₂O 1%; MgO 0.5%. The culturing soil was slightly acidic (pH 6). Samples of leaves and stem of bamboo were collected for inorganic content analysis quantitatively and qualitatively. Leaf age impacts on the silica accumulation in bamboo leaves²⁶. Therefore, mature leaves where silica concentration is stable were used in analyses. All samples were dried in a desiccator at 60 °C degrees for one week until the mass was stabilized. Before every leveling, samples were allowed to cool to room temperature. Samples of cortex of the stem and leaves were combusted for removing the organic phase at 900 °C for one hour and let to cool to room temperature before leveling and calculating the wt% quantity of the inorganic compounds. Statistical comparison between inorganic compound content of leaves and outer skin of the cortex were studied using the Wilcoxon rank sum test with values of $p < 0.05$ being considered statistically significant.

SEM–EDS analysis

For elemental and morphological characterization of the phytoliths from cortex of the stem and leaves, SEM–EDS analysis was used. To obtain a clear cross section cut, broad ion beam (BIB) sectioning was used. The applied apparatus was an Ilion+ Advantage—Precision Cross-Section System (model 693) by Gatan, USA. As BIB gives a rather small cross section area, traditional epoxy casting and sanding/polishing was applied to obtain a significantly larger cross section area. The cross section area was in total of 20.4 mm in diameter and cross-section of 10.0 mm of the leaf was visually scanned for determining interphytolith distance and size of the phytoliths.

SEM–EDS analysis was done using a Zeiss Gemini 2450 scanning electron microscope with XFlash 6|60 and XFlash 5060F X-ray analyzers. The applied voltages were between 5 and 15 V, the samples were gold-coated before SEM–EDS analysis.

RAMAN spectroscopy

To study the structure of phytoliths, especially whether they were crystalline or amorphous, RAMAN spectroscopy was applied with a Renishaw in Via Qontor confocal Raman microscope system. The used wavelength was 532 nm. Raman was selected, because of its known suitability to detect signals from crystalline Si. Also, with the applied Raman spectrometer it is possible to investigate point targets with approx. 1 µm diameter, which is well below the size of the studied leaf phytoliths. Raman spectra of quartz, tridymite and cristobalite were used as control.

TEM analysis

SEM–EDS showed that the particles containing silicon are such a small size in the cortex of the stem that their morphology was not able to be defined by SEM, therefore TEM was used for more precise morphological characterization. Bamboo PA was selected for TEM analysis. Three samples were made for TEM analysis. For fixation, bamboo samples were soaked in 0.9% saline water for 30 min. The samples were fixed with 5% glutaraldehyde in s-collidine buffer, dehydrated with ethanol, and embedded in a 45359 Fluka Epoxy Embedding Medium kit. Thin sections were cut using an ultramicrotome to thickness of 70 nm. The sections were stained

using uranyl acetate and lead citrate. The sections were examined using a JEOL JEM-1400 Plus transmission electron microscope operated at 80 kV acceleration voltage.

STEM-EDS analysis

To get a precise location of silica particles in cortex we used same samples than in TEM analysis (Figure 5A). SEM micrographs were obtained with Apreo S field-emission SEM (Thermo Scientific, The Netherlands) equipped with a Ultim Max 100 energy dispersive X-ray spectrometer (EDS; Oxford Instruments, United Kingdom). STEM images were obtained with a dedicated STEM-in-SEM detector using an acceleration voltage of 10 kV. Elemental mapping was performed using an acceleration voltage of 10 kV.

Surface microhardness indentation

Surface microhardness (in GPa) with corresponding load–vertical displacement diagrams and modulus of elasticity (in GPa) of the outer cortex and inner cortical part of the stem perpendicular to the curvature of the stem, was measured with microhardness indentation device (Rtec SMT 5000, Rtec Instruments, San Jose, CA, USA) with maximum load of 10.0 N. One millimeter thick samples of the cortex and underlying inner part of six samples were prepared from bamboos PA and PB, placed on a sample holder followed by four consecutive automatic indentations. Means of four measurements were used in the calculation of statistical differences between the hardness of the outer cortex and inner part of the stem (Wilcoxon/Kruskal–Wallis test).

Micro-CT examination

To confirm and visualize the location and distribution of phytoliths in the leaf and stem of bamboo PA, computer tomography scanning was performed. The bamboo leaves and stem were scanned with a Bruker-Skyscan 1272 micro-CT with the following settings: tube (Hamamatsu L10101) voltage 50 kV, current 200 mA. No filtering was used. Scaled pixel size 3 μm , camera pixel size 7.4 μm (2×2 binning), image size 2452×1640 pixels, rotation step 0.150 degrees. The cross-sectional images were reconstructed with NRecon program version 1.7.5.6 using the InstaRecon 2.0.4.5 engine, image smoothing 3, ring artifact reduction 15, beam hardening correction 70%, minimum attenuation to image 0.001 HU, maximum 0.100, 8-bit grayscale image output. False-color illustrations of image stacks were generated with the CTVox rendering program. Highest attenuation regions, i.e., the highest density is arbitrarily shown as blue, middle values green and low attenuation red.

Results

Combustion analysis showed that there were significantly ($p = 0.0002$) fewer inorganic compounds in the stem than in leaves of both bamboo species (PA, PB). The wt% of inorganic compounds of PB leaves was 8.0% and wt% of PB cortex was 1.3% and wt% of inorganic compounds in PA leaves was 5.8% and wt% of PA cortex was 0.9%, respectively (Fig. 1). Morphological and elemental analysis by SEM–EDS demonstrated phytolith size in the leaves to be 30–40 μm in diameter and they were located in the upper surface of the leaf with a 120 μm distance from each other (Fig. 2). The stem (culm) of the bamboo did not contain detectable phytoliths by SEM although the outer cortex of the stem had silicon containing compounds determined by EDS analysis (Fig. 3). EDS analysis of the phytoliths of leaves showed silicon to be the major element which was detected (Fig. 2). Raman spectroscopy showed an amorphous structure for the silica of the phytoliths of the leaves and silica in the cortex of the stem whereas the control material of quartz, tridymite and cristobalite showed typical Raman shift for crystal structure (Figure 7). TEM micrographs from bamboo PA showed fine granularity in the outer green part of the cortex (Figs. 4A,B and 5B) in areas where Si was detected in SEM–EDS (Fig. 6B). Absence of the granularity further away from the surface where Si was not detected by SEM–EDS (Fig. 6B) suggests that the granularity is the precipitated mineral. Nano meter size mineral precipitation of silica on the outermost cortex cells were located in the SEM–EDS analysis (Fig. 3). STEM image (Fig. 6A) showing same area in same sample than TEM image (Fig. 5A). Location of oxygen (Fig. 6C) follows same area than silicon (Fig. 6B). Surface microhardness indentation showed the hardness of the outer cortex of bamboo PA to be 0.0648 GPa and bamboo PB 0.0732 GPa, whereas corresponding values for the inner part of the stem were 0.0064 GPa and 0.0086 GPa (Table 1). The surface microhardness of the green cortex and culm differed significantly ($p < 0.0001$) (Fig. 7). The modulus of elasticity for the cortex of both species of bamboo were higher than that of the inner part of the stem (Table 1). Typical load-indentation displacement curves of surface microhardness measurement of the outer cortex and inner surface of the stem of bamboo PA and PB are shown in Fig. 8. CT scans of the leaf and cortex of the stem of the bamboo PA showed areas of higher density (blue) representing mineral precipitation which corresponds to the findings by SEM (Fig. 9). There was more mineral precipitation on the upper surface of the leaf than on the lower surface (Fig. 9A–C). Cortex of the stem showed less mineral precipitation than leaves (Fig. 9D).

Discussion

Bamboo culm have been used for millennia in traditional construction because of its excellent flexibility and toughness. The bamboo culm is composed of optimized natural unidirectional fiber-reinforced composites with cellular parenchyma as the matrix. The fibers are the major components that provide the strength and toughness of bamboo. The presence of silica phytoliths increases critical stress of random cracks in the bamboo cortex²⁷. Structural analysis of bamboo cortex has recently been made using micro-CT, and porosity of the cortex with classification of cortex cells were presented but no attention was paid to the presence and distribution of silica phytoliths in the cortex²⁸. However, phytoliths have been characterized by other means extensively. For instance, electron microscopy has been used to demonstrate phytoliths size in grass to be classifiable into two size categories: 10–20 μm and over 300 μm in size, with the latter being possibly consisting of aggregates of silica

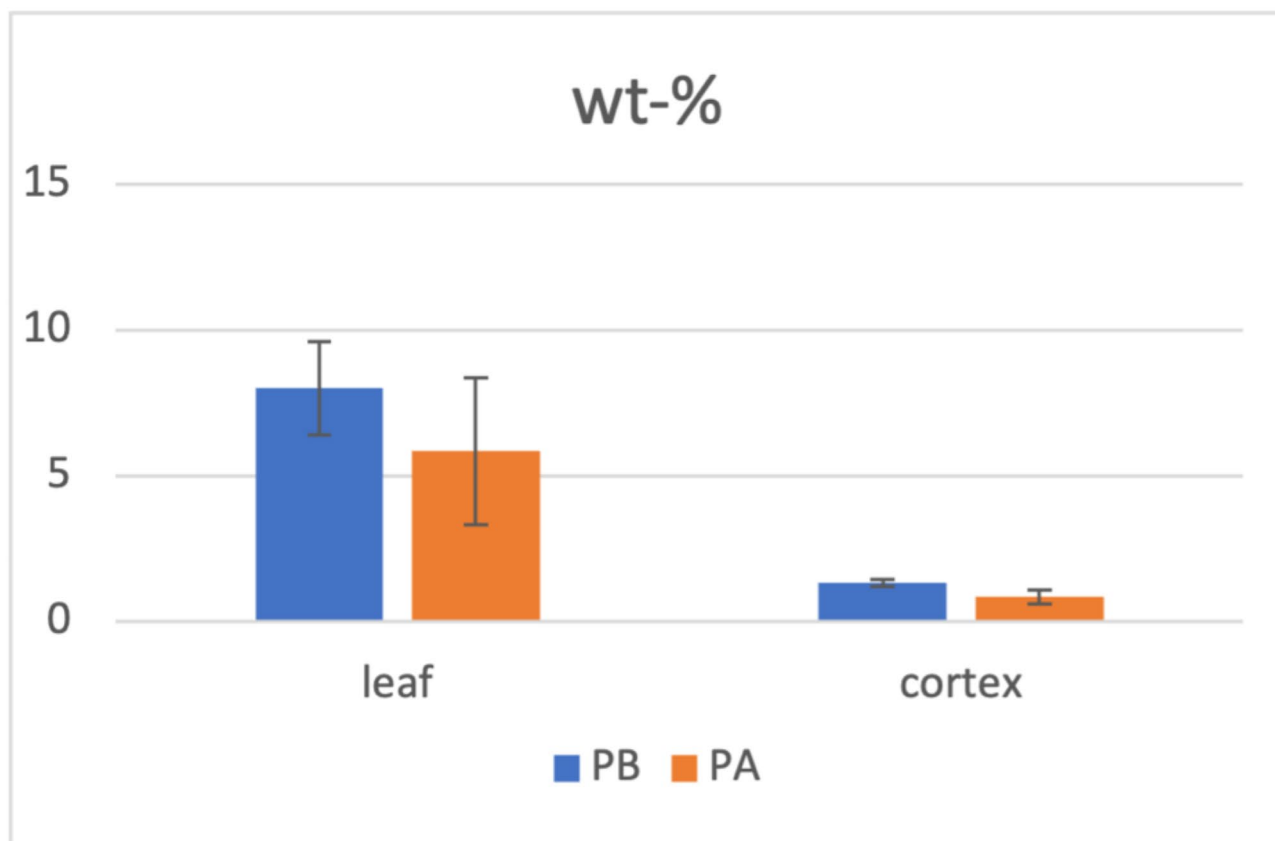


Fig. 1. wt% quantity of the inorganic compounds of leaves and cortex of stem of bamboo PA and PB.

grains²². SEM examination in our study of phytoliths of the leaves of bamboo did show any signs of aggregated structure, instead the phytoliths showed a dense and homogeneous microstructure of phytoliths although they were slightly larger than the 10–20 μm phytoliths studied by Liu et al.²².

Tooth wear of mammals by phytoliths has been of great interest historically. It was shown that phytoliths can abrade the enamel surface of teeth which has been used as tools in research on archaeology and paleoecology²⁹. The extinct hominoid *Gigantopithecus blacki* has been one of the species of interest, because of its dental proportions and tooth morphology, which in some ways resembles that of giant panda, a species whose diet consists almost entirely of bamboo³⁰. By some estimates, bamboo makes up approximately 99% of the panda's diet³¹. Both the leaves and culm of bamboo are eaten but from July to October leaves are the major part of the diet²⁵. In the wild, the giant panda's preference for a given bamboo species is highly seasonal and may be related to habitat selection. Giant pandas migrate to different altitudes in their mountainous home ranges at specific times of the year. Although this migration and diet change between habitat and bamboo species occurs, the giant panda is also alternating between the bamboo plant parts consumed. It has been shown that the leaves were eaten from January to February with culm consumption occurring in March and April²⁵. It has been speculated that the increase in lignin and cellulose in winter and spring could be cause for the decreased consumption of leaves².

For the mastication of bamboo its physical properties have an impact. One of the material properties which is considered in this context is hardness. Hardness refers to resistance to plastic deformation under stress and some comparative hardness measurements of some bamboo species (*P. bissetii*, *P. dulcis*, *P. japonica* and *P. nigra*) were made and the highest hardness (14 MPa) of the stem was for *P. bissetii*¹⁵. The values in general were close to our values of the culm of bamboo PA and PB (6.4 MPa and 8.6 MPa) whereas we found higher values for the cortex, the part of the stem which is removed by the feeding pattern (64.9 MPa and 73.3 MPa, respectively). King¹⁵ found modulus of the elasticity of the stem to be 1.5 GPa but whether the measurement was made from the cortex or culm was not reported. We found corresponding values for the cortex (1.4 GPa for PA and 1.7 GPa for PB).

Tooth wear is typically considered to be an abrasive type of wear although wear can be caused by other mechanisms too. Higher hardness of abrasive particles than hardness of the wearing substrate is required for the abrasive wear. The roles of endogenous abrasives of phytoliths, versus exogenous wind and rain born abrasives in the wear of teeth, has been debated for a long time. Hardness measurements of phytoliths suggested that wear of dental enamel might be less than previously thought^{32–34}. Surface microhardness of phytoliths is lower than hardness of tooth enamel^{33,35}. The mean value for wild boar enamel is 6.5 GPa and for bovine enamel 5.7 GPa^{36,37} whereas native phytoliths have a surface hardness of 0.75–2.38 GPa³⁵. Although values of surface microhardness suggest that abrasion of teeth may not be the cause for tooth wear, some contradictory opinions have been



Fig. 2. SEM–EDS micrograph of a leaf where phytoliths (red) are located in the upper side of the leaf. The distance between phytolith particles is 120 μm . Original magnification 441 \times , bar = 50 μm).

stated. Rabenold and Pearson³⁸ have claimed that phytoliths despite their lower surface hardness may anyhow be the principal abrasive agent for tooth wear in certain environments. Indeed, it is possible that the mineral composition and pH of the soil where the plant is growing influences the composition, quantity, structure and physical properties of phytoliths. It is known that bamboos grow the best when the soil pH is 5.5. to 7, as was the case in the soil where bamboos for the present study were grown³⁹. Rabenold and Pearson³⁸ further suggested that phytoliths appear to be a key selective force behind the evolution of thick molar enamel in primates and that the quantity of phytoliths rather than their surface hardness in food correlates with the evolution of thick molar enamel. Possible effects of pH drop by the food and related softening of the enamel may also relate to phytolith induced wear to teeth.

The giant panda's tooth enamel is analogous to human enamel in its mechanical properties⁷. In enamel as the most highly mineralized tissue in mammals the nanosized hydroxyapatite mineral crystals are glued together by protein enamelin and the formed structure contains micrometer scale units of enamel rods⁴⁰. Enamel is anisotropic with lower hardness and indentation toughness along the longitudinal direction, as compared to the transverse direction. Thus, damage is more prone to occur through plastic shearing or cracking along the sheets due to their high organic content⁴¹. The content of the hard hydroxyapatite of enamel is high on the occlusal surface and decreases continuously toward the dentin-enamel junction and this can result in an increasing wear rate by the progress of the wear^{42,43}. Structural hierarchy renders the enamel to fulfill its mechanical demand for mastication of millions of times during the lifetime of the organisms^{40,44–46}. Because the digestive system of giant pandas cannot fully utilize the nutrients in bamboo^{47,48}, pandas must continuously consume up to 20 kg bamboo per day. Constant mastication put teeth under continuous dynamic mechanical stress of different types and can affect tooth wear.

Although enamel is hard its structure has developed to resist dynamic stress concentrations by the biting cycle. Cortex of the stem of bamboo possesses a combination of high stiffness, strength and fracture toughness. Biting of tough substances causes stress between the enamel prisms and can cause localized microcracks to the enamel. Accumulation of cracks can cause material loss, i.e. tooth wear without the presence of hard abrasive particles. Wear of this type is called fatigue wear. In fact, Weng et al.⁷ in their extensive research showed that although panda enamel is superior in hardness and modulus of elasticity compared to bamboo, it is inferior

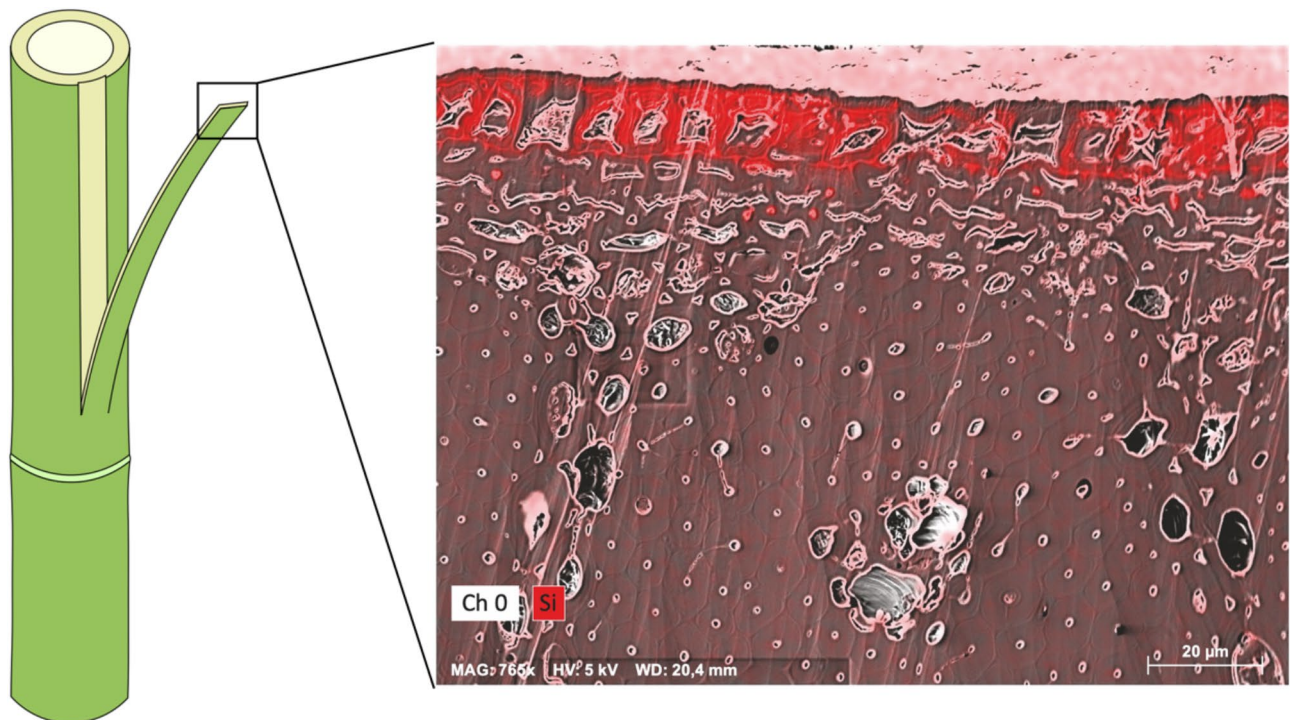


Fig. 3. Schematic view of the bamboo stem and the green cortex and corresponding SEM–EDS micrograph of the cross-section showing mineral precipitation (red) on the cortex of the stem. Original magnification 765 ×, bar = 20 µm.

in toughness. Later they²⁴ specifically examined the enamel of giant panda and demonstrated the micro-scale damage tolerance that enamel additionally generates in the tooth through the attachment of compliant dentin foundation to the enamel using a graded interface of dentin-enamel junction. Although the durability and recovery capability of the enamel of giant panda is exceptional, it is possible that wear of the fatigue type may occur and that the purpose of removing the hard and tough cortex of the bamboo stem is to protect molars from wear. Exogenous and endogenous abrasive particles probably have a synergistic role in the total wear which has several tribological mechanisms, including so-called attrition (tooth-to-tooth contact wear). More detailed research of the microstructure of giant panda premolars versus molars with different functional roles in the masticatory cycle would increase our understanding of the adaptation to a bamboo diet.

Removal of cortex of bamboo culm by giant panda takes place without exception as has been reported by Hansen et al.²⁵. Typically, the feeding panda spends sedentarily several hours daily in processing the bamboo, including the time-consuming removal of the cortex^{2,25}. This has made the panda vulnerable to hunting carnivores, like the subspecies of leopard (*Panthera pardus*) and tiger (historical range of subspecies of *Panthera tigris*). Caro et al.⁴⁹ and Nokelainen et al.⁵⁰ have recently shown that the characteristic black-and-white colour of panda is most probably a cryptic camouflage against the predators, in forest and snowy mountain habitats. Interestingly, we have observed that sitting and feeding pandas cover their white belly with the debris of peeled cortex and other parts of the discarded bamboo, further suggesting that the sedentary feeding pattern has been a critical risk by predation. In Finland (Ähtäri Zoo), the debris dropping of bamboo debris to cover white belly is somewhat more common during summertime (green camouflage) than during the snowy conditions of winter. Whether this behaviour of panda can be found their natural habitat has not been reported.

Conclusions

This study showed that the majority of phytoliths were located in the leaves of bamboo and that the phytoliths were amorphous silica in their chemical composition. Species PA and PB did not differ in these respects from each other. It can be expected that the feeding pattern to remove the cortex of the stem before eating relates to hardness of the cortex and that phytoliths may be a synergistic causative factor of tooth wear in giant panda in certain parts of their dentition.

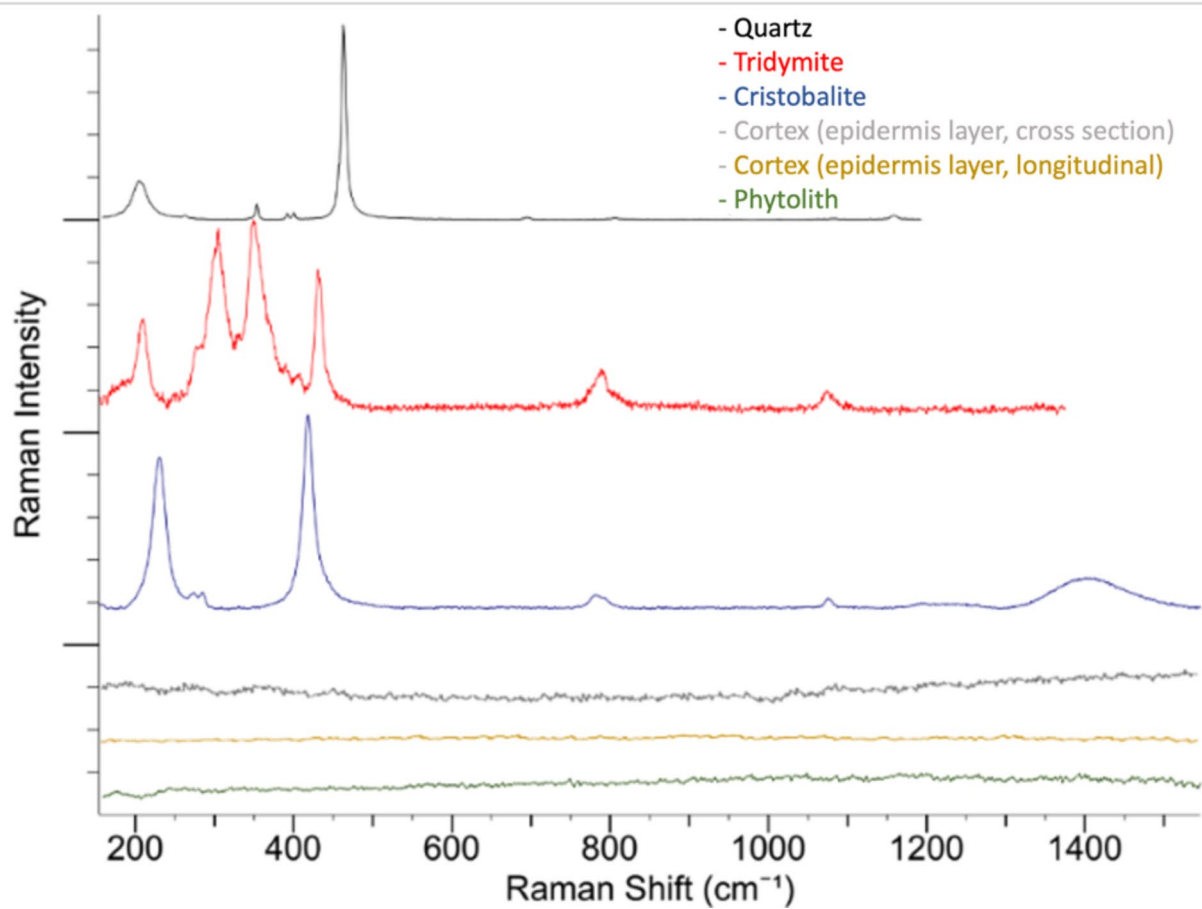


Fig. 7. RAMAN spectra of reference of quartz, tridymite and cristobalite showing typical Raman shift for the crystal structure. Gray and yellow lines are showing amorphous structure of precipitation of silica in bamboo cortex and underlying epidermis layer of the stem. Green line shows amorphous structure of phytolith from leaf.

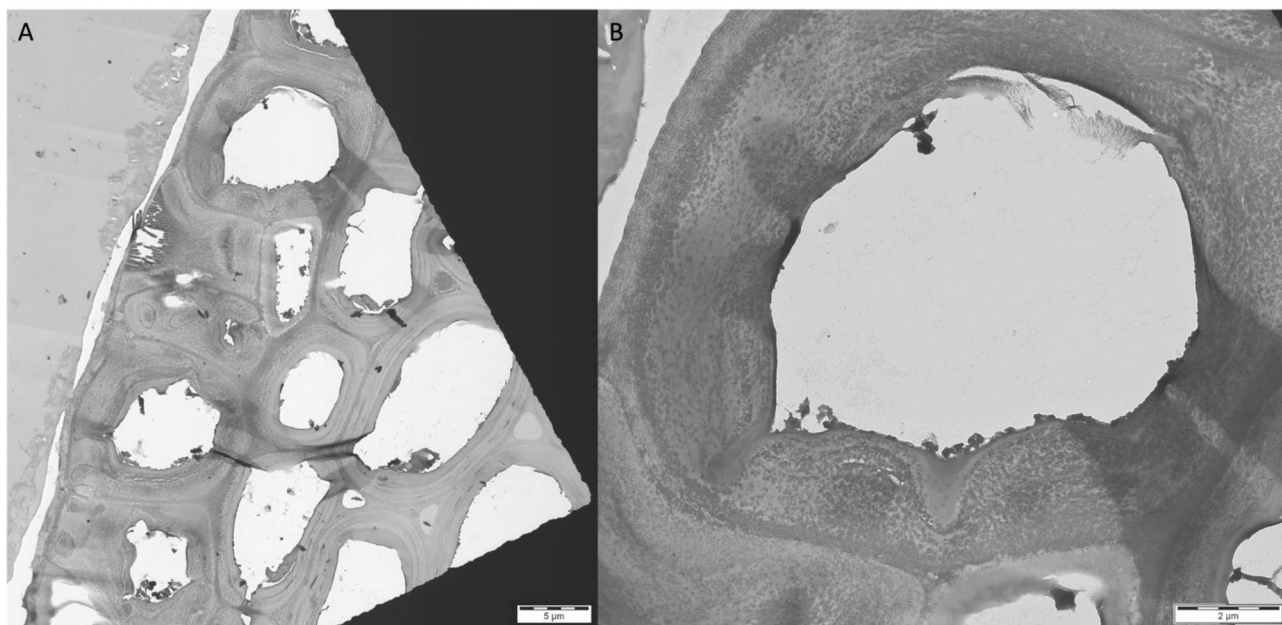


Fig. 4. TEM micrograph of cross section of the green cortex of the stem of bamboo PA. On the right with original magnification $800\times$ (bar = $5\mu\text{m}$) and with higher magnification (original magnification $3000\times$, bar = $2\mu\text{m}$). Dark grey areas represent precipitation of nanometer scale mineral precipitation.

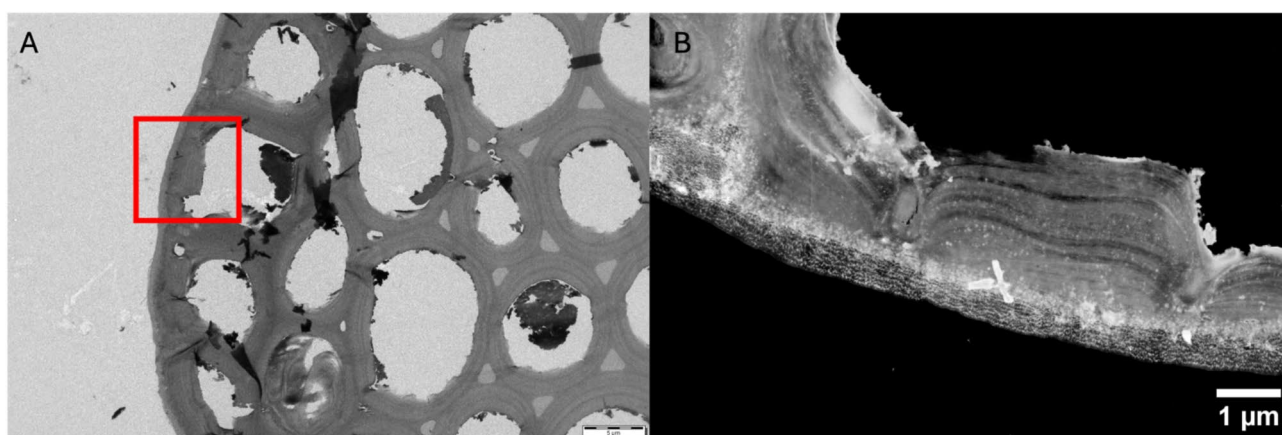


Fig. 5. A TEM micrograph of bamboo cortex, B STEM high angle annular dark field micrograph of outer layer of bamboo cortex. White spots represent heavier elements.

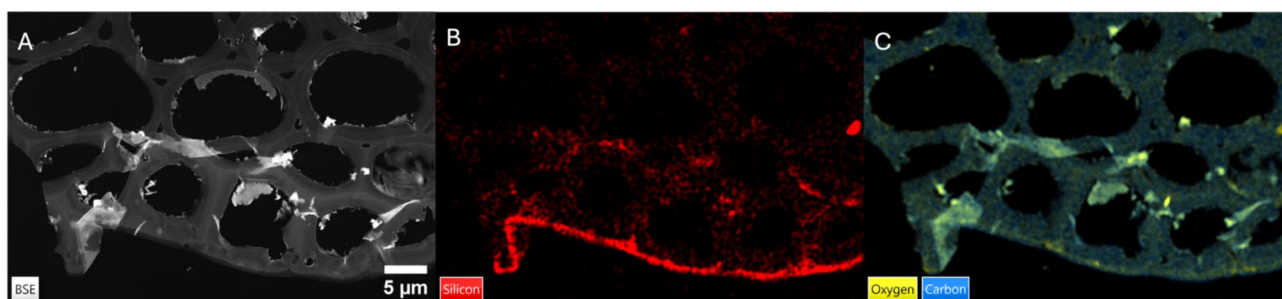


Fig. 6. A BSE (backscattered electrons) micrographs of cortex of bamboo. EDS micrographs from same area than Fig. 5 A. B showing presence of silicon on the cortex. C showing oxygen and carbon location on bamboo cortex.

	Micro hardness	Modulus of elasticity
PA cortex	0.0648 (+/- 0.0073) ^a	1.4023 (+/- 0.1389) ^c
PA culm	0.0064 (+/- 0.0005) ^a	0.3986 (+/- 0.0408) ^c
PB cortex	0.0732 (+/- 0.0087) ^b	1.7235 (+/- 0.2583) ^d
PB culm	0.0086 (+/- 0.0011) ^b	0.3315 (+/- 0.0769) ^d

Table 1. Surface microhardness (GPa) and modulus of elasticity (GPa) (+/-SD) of the green cortex and inner part of the stem (culm) of bamboo PA and PB. Values marked with superscript differed statistically significantly ($p < 0.0001$).

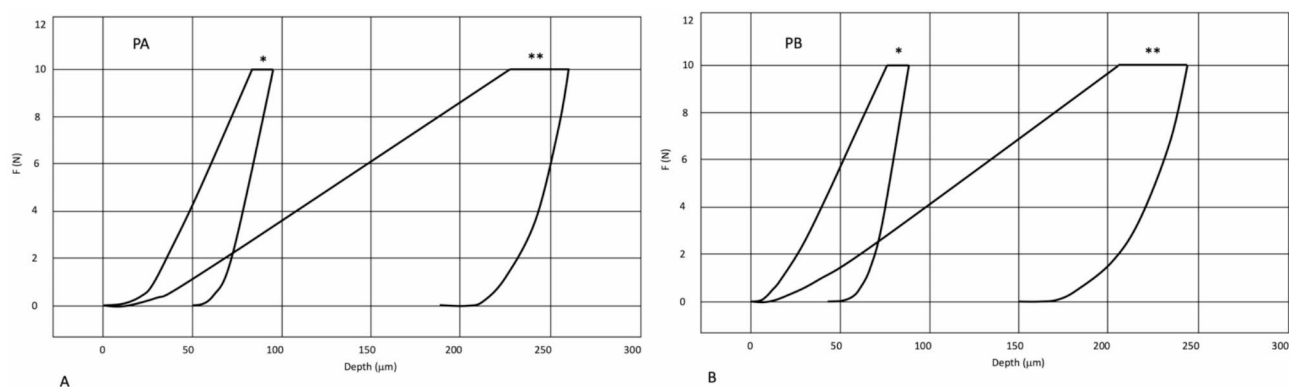


Fig. 8. Load–displacement curve of surface microhardness. (A) Bamboo PA; (B) bamboo PB. * refers indentation of outer cortex and ** inner part of the stem.

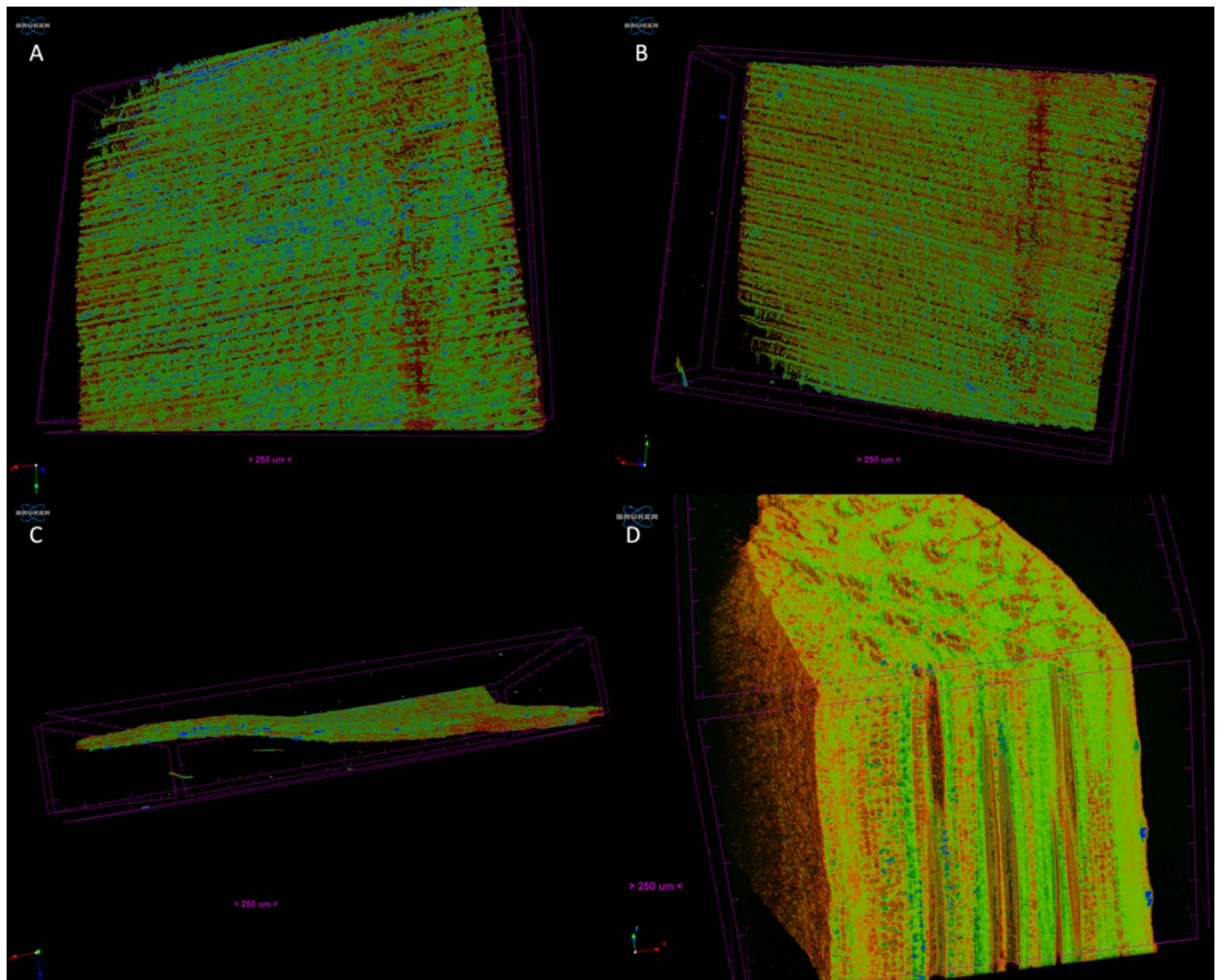


Fig. 9. CT-scans of bamboo PA. Leaf: (A) upper surface, (B) lower surface, (C) cross-section and (D) stem. PA. Blue areas represent areas of high density phytoliths. Bar = 250 µm.

Data availability

The authors declare that the data supporting the findings of this study are available within the paper and its Supplementary Information files. Should any raw data files be needed in another format they are available from the corresponding author upon reasonable request.

Received: 21 August 2024; Accepted: 18 March 2025

Published online: 02 April 2025

References

- Schaller, G. B., Jinchu, H., Wenshi, P. & Jing, Z. *The Giant Pandas of Wolong* (University of Chicago Press, 1985).
- Long, Y. et al. Nutritional strategy of giant pandas in the Qinling mountains of China. In *Giant Pandas—Biology and Conservation* (eds Lindburg, D. & Baragona, K.) 90–100 (University of California Press, 2004).
- Nie, Y. et al. Exceptionally low daily energy expenditure in the bamboo-eating giant panda. *Science* **349**, 171–174 (2015).
- Vallittu, P. K. et al. Temporomandibular joint and Giant Panda's (*Ailuropoda melanoleuca*) adaptation to bamboo diet. *Sci. Rep.* **11**, 14252 (2021).
- Jain, S., Kumar, R. & Jindal, U. C. Mechanical behaviour of bamboo and bamboo composite. *J. Mater. Sci.* **27**, 4598–4604 (1992).
- Tan, T. et al. Mechanical properties of functionally graded hierarchical bamboo structures. *Acta Biomater.* **7**, 3796–3803 (2011).
- Weng, Z. Y. et al. Giant panda's tooth enamel: Structure, mechanical behavior and toughening mechanisms under indentation. *J. Mech. Behav. Biomed. Mater.* **64**, 125–138 (2016).
- Gu, Y., Liu, H., Wang, H., Li, R. & Yu, J. Phytoliths as a method of identification for three genera of woody bamboos (Bambusoideae) in tropical southwest China. *J. Archaeol. Sci.* **68**, 46–53 (2016).
- Parsons, J. L. Bamboo nutritional composition, biomass production, and palatability to giant pandas: disturbance and temporal effects. Thesis, UMI Number 3590228. (Mississippi State University, 2013).
- Zhu, L., Wu, Q., Dai, J., Zhang, S. & Wei, F. Evidence of cellulose metabolism by the giant panda gut microbiome. *Proc. Natl. Acad. Sci.* **108**, 17714–17719 (2011).
- Yin, X. et al. Further understanding of the silicon morphological fundamentals of bamboo culm. *BioRes* **11**, 10329–10338 (2016).

12. McNaughton, S. J. & Tarrants, J. L. Grass leaf silicification: Natural selection for an inducible defense against herbivores. *Proc. Natl. Acad. Sci.* **80**, 790–791 (1983).
13. Vicari, M. & Bazely, D. R. Do grasses fight back? The case for antiherbivore defences. *Trends Ecol. Evol.* **8**, 137–141 (1993).
14. Massey, F. P., Roland Ennos, A. & Hartley, S. E. Herbivore specific induction of silica-based plant defences. *Oecologia* **152**, 677–683 (2007).
15. King, R. A. Using *Ailuropoda melanoleuca* as a model species for studying the ecomorphology of *Paranthropus*. Marshall University, Theses, dissertations and capstones. Paper 874. (Marshall University, 2014).
16. Lucas, P. W., Turner, I. M., Dominy, N. J. & Yamashita, N. Mechanical defences to herbivory. *Ann. Bot.* **86**, 913–920 (2000).
17. Massey, F. P. & Hartley, S. E. Experimental demonstration of the antiherbivore effects of silica in grasses: Impacts on foliage digestibility and vole growth rates. *Proc. R. Soc. B* **273**, 2299–2304 (2006).
18. Carnelli, A. L., Madella, M. & Theurillat, J.-P. Biogenic silica production in selected alpine plant species and plant communities. *Ann. Bot.* **87**, 425–434 (2001).
19. Hodson, M. J., White, P. J., Mead, A. & Broadley, M. R. Phylogenetic variation in the silicon composition of plants. *Ann. Bot.* **96**, 1027–1046 (2005).
20. Piperno, D. R. *Phytolith Analysis: An Archaeological and Geological Perspective* (Academic Press, 1988).
21. Ciochon, R. L., Piperno, D. R. & Thompson, R. G. Opal phytoliths found on the teeth of the extinct ape *Gigantopithecus blacki*: Implications for paleodietary studies. *Proc. Natl. Acad. Sci. U.S.A.* **87**, 8120–8124 (1990).
22. Liu, H. et al. Dissolution does not affect grass phytolith assemblages. *Palaeogeogr. Palaeoclimatol. Palaeoecol.* **610**, 111345 (2023).
23. Suzuki, S., Suzuki, S. H. & Cox, C. F. Evaluating the antagonistic wear of restorative materials when placed against human enamel. *J. Am. Dent. Assoc.* **127**, 74–80 (1996).
24. Liu, Z. et al. Hydration-induced nano- to micro-scale self-recovery of the tooth enamel of the giant panda. *Acta Biomater.* **81**, 267–277 (2018).
25. Hansen, R. L. et al. Seasonal shifts in giant panda feeding behavior: Relationships to bamboo plant part consumption. *Zoo Biol.* **29**, 470–483 (2010).
26. Rotmuenwai, N., Aryuyo, K., Kruethaworn, N., Wattananit, W. & Yookongkaew, N. Exploring silica accumulation in bamboo leaves: A study on phytolith morphology and epidermal patterning in the tropical giant bamboo *Dendrocalamus copelandii*. *Ann. Bot.* **20**, 1–11 (2024).
27. Cui, J., Jiang, M., Nicola, M., Masic, A. & Qin, Z. Multiscale understanding in fracture resistance of bamboo skin. *Extreme Mech. Lett.* **49**, 101480 (2021).
28. Wang, X. et al. Quantitative characterization of bamboo cortex structure based on X-ray microtomography. *Cellulose* **29**, 4335–4346 (2022).
29. Walker, A., Hoeck, H. N. & Perez, L. Microwear of mammalian teeth as an indicator of diet. *Science* **201**, 908–910 (1978).
30. White, T. D. Geomorphology to paleoecology: *Gigantopithecus* reappraised. *J. Hum. Evol.* **4**, 219–233 (1975).
31. Wei, F., Feng, Z., Wang, Z. & Li, M. Feeding strategy and resource partitioning between giant and red pandas. *Mammalia* **63**, 417–430 (1999).
32. Lucas, P. W. et al. Mechanisms and causes of wear in tooth enamel: Implications for hominin diets. *J. R. Soc. Interface* **10**, 20120923 (2013).
33. Sanson, G. D., Kerr, S. A. & Gross, K. A. Do silica phytoliths really wear mammalian teeth?. *J. Archaeol. Sci.* **34**, 526–531 (2007).
34. Baker, G., Jones, L. H. P. & Wardrop, I. D. Cause of wear in sheep's teeth. *Nature* **184**, 1583–1584 (1959).
35. Kaiser, T. M., Braune, C., Kalinka, G. & Schulz-Kornas, E. Nano-indentation of native phytoliths and dental tissues: Implications for herbivore-plant combat and dental wear proxies. *EvolSyst* **2**, 55–63 (2018).
36. Willems, G., Celis, J. P., Lambrechts, P., Braem, M. & Vanherle, G. Hardness and Young's modulus determined by nanoindentation technique of filler particles of dental restorative materials compared with human enamel. *J. Biomed. Mater. Res.* **27**, 747–755 (1993).
37. Ang, S. F., Bortel, E. L., Swain, M. V., Klocke, A. & Schneider, G. A. Size-dependent elastic/inelastic behavior of enamel over millimeter and nanometer length scales. *Biomaterials* **31**, 1955–1963 (2010).
38. Rabenold, D. & Pearson, O. M. Abrasive, silica phytoliths and the evolution of thick molar enamel in primates, with implications for the diet of *Paranthropus boisei*. *PLoS ONE* **6**, e28379 (2011).
39. Ouyang, M. et al. Moso bamboo (*Phyllostachys edulis*) invasion increases forest soil pH in subtropical China. *CATENA* **215**, 106339 (2022).
40. Cui, F.-Z. & Ge, J. New observations of the hierarchical structure of human enamel, from nanoscale to microscale. *J. Tissue Eng. Regen. Med.* **1**, 185–191 (2007).
41. Bechtle, S. et al. Crack arrest within teeth at the dentinoenamel junction caused by elastic modulus mismatch. *Biomaterials* **31**, 4238–4247 (2010).
42. Cuy, J. L., Mann, A. B., Livi, K. J., Teaford, M. F. & Weihs, T. P. Nanoindentation mapping of the mechanical properties of human molar tooth enamel. *Arch. Oral Biol.* **47**, 281–291 (2002).
43. Xu, C., Reed, R., Gorski, J. P., Wang, Y. & Walker, M. P. The distribution of carbonate in enamel and its correlation with structure and mechanical properties. *J. Mater. Sci.* **47**, 8035–8043 (2012).
44. Macho, G. A., Jiang, Y. & Spears, I. R. Enamel microstructure—A truly three-dimensional structure. *J. Hum. Evol.* **45**, 81–90 (2003).
45. Bajaj, D., Nazari, A., Eidelman, N. & Arola, D. D. A comparison of fatigue crack growth in human enamel and hydroxyapatite. *Biomaterials* **29**, 4847–4854 (2008).
46. He, L. H. & Swain, M. V. Understanding the mechanical behaviour of human enamel from its structural and compositional characteristics. *J. Mech. Behav. Biomed. Mater.* **1**, 18–29 (2008).
47. Nie, Y. et al. Giant pandas are macronutritional carnivores. *Curr. Biol.* **29**, 1677–1682.e2 (2019).
48. Guo, W. et al. The carnivorous digestive system and bamboo diet of giant pandas may shape their low gut bacterial diversity. *Conserv. Physiol.* **8**, 104 (2020).
49. Caro, T., Walker, H., Rossman, Z., Hendrix, M. & Stankowich, T. Why is the giant panda black and white?. *Behav. Ecol.* **28**, 657–667 (2017).
50. Nokelainen, O., Scott-Samuel, N. E., Nie, Y., Wei, F. & Caro, T. The giant panda is cryptic. *Sci. Rep.* **11**, 21287 (2021).

Acknowledgements

SEM-EDS and RAMAN analyses were carried out at Top Analytica Ltd (Turku, Finland) by Eero Itälä. TEM analysis was performed at the University of Turku by Teemu Paunikallio. Electron microscopy samples were processed and TEM imaging performed in the Laboratory of Electron Microscopy, Institute of Biomedicine, University of Turku, which receives financial support from Biocenter Finland. We acknowledge the Materials Research Infrastructure (MARI) at Department of Physics and Astronomy, University of Turku for access and support with the SEM facilities. Study was supported by grants of the Academy of Finland (#357142) and Business Finland (11/31/2023).

Author contributions

J.T. and J.M.: Conducting experimental parts of the study and manuscript writing. J.V., J.S., H.Z., P.N. and M.H.: Writing manuscript from their fields of scientific expertise. J.S. acquisition of bamboo material. P.K.V.: Creating study hypothesis, planning the experimental design for the study and directing manuscript writing.

Competing interests

The authors declare no competing interests.

Additional information

Supplementary Information The online version contains supplementary material available at <https://doi.org/10.1038/s41598-025-95042-6>.

Correspondence and requests for materials should be addressed to J.T.

Reprints and permissions information is available at www.nature.com/reprints.

Publisher's note Springer Nature remains neutral with regard to jurisdictional claims in published maps and institutional affiliations.

Open Access This article is licensed under a Creative Commons Attribution-NonCommercial-NoDerivatives 4.0 International License, which permits any non-commercial use, sharing, distribution and reproduction in any medium or format, as long as you give appropriate credit to the original author(s) and the source, provide a link to the Creative Commons licence, and indicate if you modified the licensed material. You do not have permission under this licence to share adapted material derived from this article or parts of it. The images or other third party material in this article are included in the article's Creative Commons licence, unless indicated otherwise in a credit line to the material. If material is not included in the article's Creative Commons licence and your intended use is not permitted by statutory regulation or exceeds the permitted use, you will need to obtain permission directly from the copyright holder. To view a copy of this licence, visit <http://creativecommons.org/licenses/by-nc-nd/4.0/>.

© The Author(s) 2025